Hydraulic Design of Stepped Spillways and Downstream Energy Dissipators for Embankment Dams

Carlos A. Gonzalez and Hubert Chanson
Div. of Civil Engineering, The University of Queensland, Brisbane QLD 4072, Australia
Ph.: (61 7) 3365 3516 - Fax: (61 7) 3365 4599 - E-mail: h.chanson@uq.edu.au

Keywords: stepped spillways, skimming flows, embankment dams, air entrainment, flow resistance, hydraulic design, energy dissipation.

Abstract
In recent years, the design flows of many dams were re-evaluated, often resulting in discharges larger than the original design. In many cases, the occurrence of the revised flows could result in dam overtopping because of insufficient storage and spillway capacity. An experimental study was conducted herein to gain a better understanding of the flow properties in stepped chutes with slopes typical of embankment dams. The work was based upon a Froude similitude in large-size experimental facilities. A total of 10 configurations were tested including smooth steps, steps equipped with devices to enhance energy dissipation and rough steps. The present results yield a new design procedure. The design method includes some key issues not foreseen in prior studies : e.g., gradually varied flow, type of flow regime, flow resistance. It is believed that the outcomes are valid for a wide range of chute geometry and flow conditions typical of embankment chutes.

Introduction

In recent years, the design flows of many dams were re-evaluated, often resulting in discharges larger than the original design. In many cases, the occurrence of the revised discharges would result in dam overtopping because of insufficient storage and spillway capacity. The embankment dams are more prone to overtopping failure than other types of dams because of breaching or erosion of the downstream face of the embankment. Despite the catastrophic effects of failure, dam overtopping constitutes the majority of identified dam failures. Before the 1980s, overtopping counter-measures consisted mainly of increasing the reservoir storage or spillway capacity. Lately overtopping protection systems have gained acceptance because they safely allow controlled flows over the dam wall during large flood events (Fig. 1).

There are several techniques to armour embankment slopes, including paving, rip-rap gabions, reinforced earth, pre-cast concrete slabs and roller compacted concrete (RCC). RCC protection and gabion placement techniques yield embankment protections shaped in a stepped fashion. While most modern stepped spillways are designed as prismatic rectangular chutes with horizontal steps, recent studies suggested different step configurations that might enhance the rate of energy dissipation (Andre et al. 2004, Chanson and Gonzalez 2004). Some older structures were equipped with devices to enhance energy dissipation: some had pooled

steps with vertical walls (Sorpe dam, 1932) or rounded end sills (Le Pont dam, 1882) (Fig. 2). Macro-roughness systems consisting of concrete blocks were studied also (Manso and Schleiss 2002).

All the above-mentioned techniques may effectively enhance the flow resistance, but their attractiveness is counterbalanced by the increased structural loads to the chute and the needs of extraordinary placement methods that might increase the construction period and total costs. Hence, more effective methods to increase the energy dissipation of embankment overflows are needed. This study review a series of experimental investigation of the hydraulic performance of moderate-slope stepped chutes with flat smooth steps, rough steps and of chutes equipped with different configurations of longitudinal ribs acting as turbulence manipulators (Fig. 2). The results aim to understand the turbulent energy dissipation processes occurring down the stepped chutes. They also provide new, original insights into air-water stepped spillway flows not foreseen in prior studies and they yield new design criteria for stepped chutes with moderate slopes typical of embankment dams ($15° < \theta < 25°$).

Experimental investigations

Experimental channel

New experiments were conducted at the University of Queensland in a 3.6 m long, 1 m wide chute with flow rates ranging from 0.10 to 0.19 m^3/s corresponding to the skimming flow regime. Two chute slopes (16 and 22°) and two step heights (h = 0.05 & 0.1 m) were tested, but the most comprehensive experiments were conducted with the 22° chute with 0.1 m step height (Table 1).

The water supply pump was controlled by an adjustable frequency motor, allowing an accurate control of the closed circuit system. Waters were fed from a large basin (1.5 m deep, 6.8×4.8 m^2 area) leading to a convergent sidewall with a 4.8:1 contraction ratio. The test section consisted of a broad-crested weir (1 m wide, 0.6 m long, with upstream rounded corner) followed by ten steps (h = 0.1 m) or 18 steps (h = 0.05 m). The stepped chute was 1 m wide with perspex sidewalls followed by a horizontal canal and a dissipation pit. With the 22° slope, ten stepped geometries were tested systematically with several flow rates (Fig. 2, Table 1). The first configuration had ten flat smooth horizontal steps. In the second, third, fourth, fifth, sixth and seventh configurations, some longitudinal ribs were placed across the step cavity from steps 2 to 10 as illustrated in Figure 2. The triangular vanes (0.1 m by 0.25 m) were made of thin aluminium plates, and they did not interfere with the free-stream. The second and fourth configurations had respectively 3 and 7 vanes placed in line, the third and fifth configurations had 3 and 7 vanes placed in zigzag. The sixth configuration had 7 in line vanes per step every two steps, while the seventh configuration had 7 vanes per step set in zigzag every two steps.

Fig. 1 - Embankment dam stepped spillways

(A) Stepped spillway of the Opuha embankment dam (Courtesy of Tonkin and Taylor, NZ)

(B) Melton dam secondary spillway (Australia)

For the last three geometries (configurations 8, 9 and 10), the step faces were covered with rough plastic square-patterned screens (8 mm high). In configuration 8, the rough screens covered both the vertical and horizontal step faces. In configuration 9, only the vertical step faces were covered, while only the horizontal ones were covered in configuration 10. The hydraulic roughness of the screens was tested independently in a 20 m long, 0.25 m wide tilting flume with glass sidewalls (Gonzalez et al. 2005). The resulting equivalent Darcy friction factor of the screens ranged from f_{screen} = 0.05 to 0.08, corresponding to a Gauckler-Manning coefficient of about 0.016 to 0.02 s/m$^{1/3}$. The results were basically independent of Reynolds number and the data were best correlated by:

$$\frac{1}{\sqrt{f_{screen}}} = 0.252 \times \left(\frac{k}{D_H} \right)^{-0.823} \quad [1]$$

with a normalised correlation coefficient of 0.783, where k is the screen height (k = 8 mm) and D_H is the hydraulic diameter.

Further details on the experiments are reported in Gonzalez (2005) and Gonzalez et al. (2005).

Instrumentation and data processing

Clear-water flow depths were measured with a point gauge. The flow rate was deduced from the measured upstream head above crest, after a detailed in-situ calibration (Gonzalez 2005).

The air-water flow properties were measured with a double-tip conductivity probe (∅ = 0.025 mm). The double-tip conductivity probe was designed with both sensors aligned in the flow direction. The leading tip had a small frontal area (0.05 mm^2) and the trailing tip was offset to avoid wake disturbance from the first tip. An air bubble detector excited the probe. Its output signal was scanned at 20 kHz for 20 s per probe sensor. The translation of the probes normal to the flow direction was controlled by a fine adjustment traveling mechanism connected to a Mitutoyo™ digimatic scale unit. The error on the vertical position of the probe was less than 0.025 mm. The accuracy on the longitudinal probe position was estimated as Δx < +/- 0.5 cm. The accuracy on the transverse position of the probe was less than 1 mm.

Table 1 - Summary of detailed experimental investigations on moderate slope stepped chutes

Reference	Slope θ deg.	Step height h m	Discharge q_w m^2/s	Geometry	Remarks
Chanson and Toombes (2002)	15.9	0.1	0.05 to 0.26	Smooth horizontal steps	W = 1 m.
	21.8	0.1	0.04 to 0.18		
Gonzalez and Chanson (2004)	15.9	0.05	0.02 to 0.20	Smooth horizontal steps	W = 1 m.
		0.1	0.075 to 0.22		
Gonzalez and Chanson (2005)	21.8	0.1	0.10 to 0.19	Smooth horizontal steps	W = 1 m.
Configuration 1				b = W = 1 m (no vane)	No vane.
Configuration 2				b = W/4 = 0.25 m (in-line)	3 vanes in-line.
Configuration 3				b = W/4 = 0.25 m (zigzag)	3 vanes in zigzag.
Configuration 4				b = W/8 = 0.125 m (in-line)	7 vanes in-line.
Configuration 5				b = W/8 = 0.125 m (zigzag)	7 vanes in zigzag.
Configuration 6				b = W/8 = 0.125 m (in-line)	7 vanes in-line every 2 steps.
Configuration 7				b = W/8 = 0.125 m (zigzag)	7 vanes in zigzag every 2 steps.
Gonzalez et al. (2005)	21.8	0.1	0.10 to 0.19	Rough horizontal steps (no vane)	W = 1 m.
Configuration 8				Rough screens on vertical & horizontal step faces	k = 8.8 mm.
Configuration 9				Rough screens on vertical step faces	k = 8.8 mm.
Configuration 10				Rough screens on horizontal step faces	k = 8.8 mm.

Fig. 2 - Examples of step configurations to enhance energy dissipation

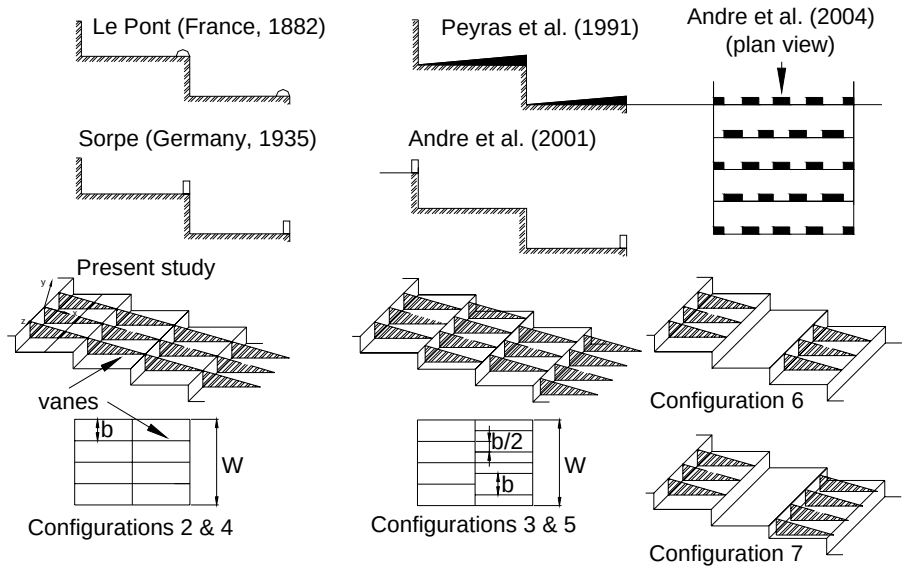

For each configuration, experiments were repeated systematically for several flow rates (Table 1). Measurements were conducted with the probe located at each step edge downstream of the inception point of free-surface aeration and at several longitudinal positions between adjacent step edges (i.e. above the recirculation cavity). For the configurations 2 to 7 with vanes, the measurements were also performed with the probe located at several transverse positions (z/b = 0 [above vanes], 0.25 and 0.5) where b is the spacing between vanes and z is the transverse direction (Fig. 2). A total of more than 330 vertical profiles were recorded with a minimum of 25 measurements per profile.

The basic probe outputs were the void fraction, bubble count rate, velocity, turbulence intensity and air/water chord size distributions. The void fraction C is the proportion of time that the probe tip is in the air. The bubble count rate F is the number of bubbles impacting the probe tip per second.

With a dual-tip probe design, the velocity measurement is based upon the successive detection of air-water interfaces by the two tips. Herein the velocity was calculated using a cross-correlation technique (Crowe et al. 1998). The time-averaged air-water velocity equals:

$$V = \frac{\Delta x}{T} \qquad [2]$$

where Δx is the distance between tips and T is the time for which the cross-correlation function is maximum. The turbulence level Tu was derived from the broadening of the cross-correlation function compared to the autocorrelation function (Chanson and Toombes 2002) :

$$Tu = 0.851 \cdot \sqrt{\frac{\Delta T^2 - \Delta t^2}{T}} \qquad [3]$$

where ΔT is a time scale satisfying : R_{xy} (T+ΔT) = 0.5*R_{xy}(T), R_{xy} is the normalised cross-correlation function, and Δt is the characteristic time for which the normalised autocorrelation function R_{xx} equals 0.5. Physically, a narrow cross-correlation function corresponds to small fluctuations in velocity, hence a small turbulence level. Conversely, a broad cross-correlation function implies large turbulence. The turbulence Tu is not a point measurement but a spatial average between probe sensors. In low volume fractions, it is equal to the turbulence intensity u'/V. Tu might not be equal to the "true" turbulence intensity, but it is an expression of some turbulence level or average velocity fluctuations (Chanson and Toombes 2002).

Basic flow patterns and flow regimes

The flow over a stepped cascade may be divided into three distinct flow regimes depending upon the flow rate for a given stepped chute geometry: nappe, transition and skimming flow regimes with increasing flow rates. The nappe flows are observed for small dimensionless discharge d_c/h where d_c is the critical flow depth and h is the step height. They are characterised by a succession of free-falling nappes at each step edge, followed by nappe impact on the downstream step. The transition flows are observed for intermediate discharges. Strong hydrodynamic fluctuations, splashing and spray near the free surface are the main features of this flow regime. Different sized air cavities alternating with fluid-filled recirculation vortices were observed between step edges below the mainstream of the flow. To date, the transition flow properties cannot be predicted accurately as very little information is available (Chanson and Toombes 2004).

The skimming flow regime is observed for the largest discharges. The water skims over the pseudo-bottom formed by the step edges as a coherent stream. Beneath the pseudo-bottom intense recirculation vortices fill the cavities between all step edges (Chamani and Rajaratnam 1999). These recirculation eddies are maintained by the transmission of shear stress from the mainstream and contribute significantly to the energy dissipation. During the present study with the Configuration 1, visual inspections highlighted the existence of three to four spanwise recirculation cells across the channel width. The findings were consistent with observations by Matos and Yasuda (Pers.comm.) on steeper chutes.

For stepped chutes with flat to moderate slopes, Chanson (1995,2001) and Ohtsu et al. (2004) proposed a further subdivision of skimming flows: a sub-regime SK1 for the lowest range of discharges and a sub-regime SK2 for the upper range. In the sub-regime SK1, a wake forms downstream of each step edge with a recirculating vortex underneath. The wake and the vortex do not extend over the full step length, and the water impacts in the horizontal part of the step. Skin friction drag occurs on the horizontal step face. For the sub-regime SK2, the wake and the recirculating eddy region extend the full length of the step sometimes interfering with the developing wake of the subsequent step. The water surface is parallel to the pseudo-bottom formed by the step edges most of the time.

Figure 3 summarises the criteria provided by Chanson (2001) and Ohtsu et al. (2004) to predict the changes in flow regimes on stepped chutes depending upon discharge and step geometry. They are based on large-size experiments, and they are expected to be applicable to prototype stepped spillways. The results were valid for all ten configurations including with rough steps and steps equipped with ribs.

Fig. 3 - Prediction of flow regime on stepped chutes

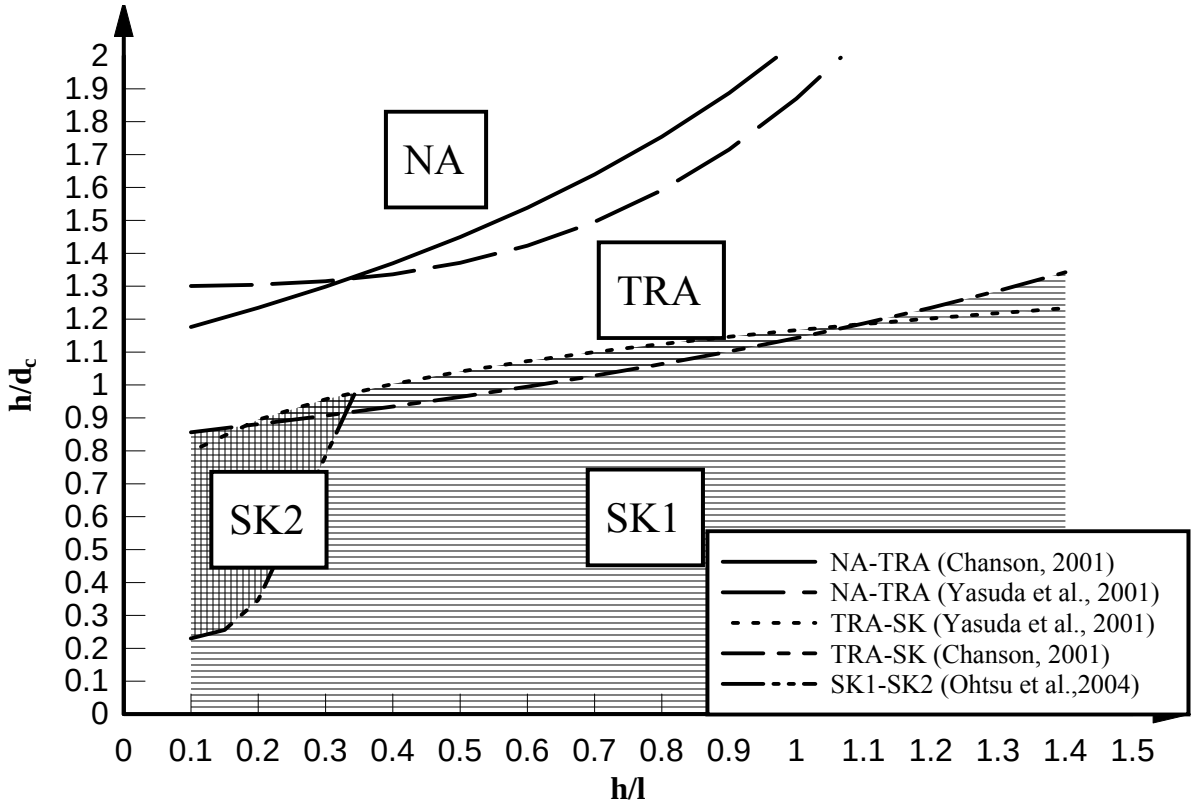

Inception point of free-surface aeration

Modern stepped spillways are designed for the skimming flow regime (Chanson 2001, Ohtsu et al. 2004, Gonzalez 2005). Skimming flows cascading down a stepped chute with smooth step faces are highly turbulent self-aerated flows. They look similar to self-aerated flows down smooth chutes. At the upstream end, the flow is smooth and transparent. When the outer edge of the developing bottom boundary layer reaches the free surface, turbulence induces strong aeration. Downstream the turbulence next to the free-surface becomes large enough to initiate natural free surface aeration (Fig. 1A).

The location of the inception point L_I is primarily a function of the discharge and the step roughness. A statistical analysis of model and prototype data yielded :

$$\frac{L_I}{h \times \cos\theta} = 9.72 \times (\sin\theta)^{0.080} \times F_*^{0.71} \quad [4]$$

where θ is the angle between the horizontal and the pseudo-bottom formed by the step edges, and F_* is :

$$F_* = \frac{q_w}{\sqrt{g \times \sin\theta \times (h \times \cos\theta)^3}} \quad [5]$$

with q_w the water discharge per unit width and g the gravity acceleration. Equation [4] was first proposed by Chanson (1995), and it is valid for skimming flows on steep spillways and embankment chutes (Chanson and Toombes 2002b, Gonzalez and Chanson 2004). Note that Equation (4) was developed for un-controlled spillway chutes. Chanson (20006) illustrated the effects of the inflow conditions on the location of the

inception point.

A comparison between smooth and rough stepped chute data is presented in Figure 4. Experimental data are compared with Equation [4] calculated for θ = 22°. The results indicated that the inception point distance from the crest L_I was approximately 35% greater for rough step faced chutes. The findings suggested a "slower" turbulent boundary layer growth on rough stepped inverts and consequently a lesser rate of energy dissipation in the clear-water flow region. Such a result is counter-intuitive compared to smooth-invert chute flows where an increased bed roughness is associated with a shorter clear-water flow region (Wood et al. 1983).

Fig. 4 - Location of the inception point of free-surface aeration - Comparison between smooth stepped chutes (black symbols, θ = 16 & 22°), rough stepped chutes (white symbols, θ = 22°) and Equation [4] (θ = 22°)

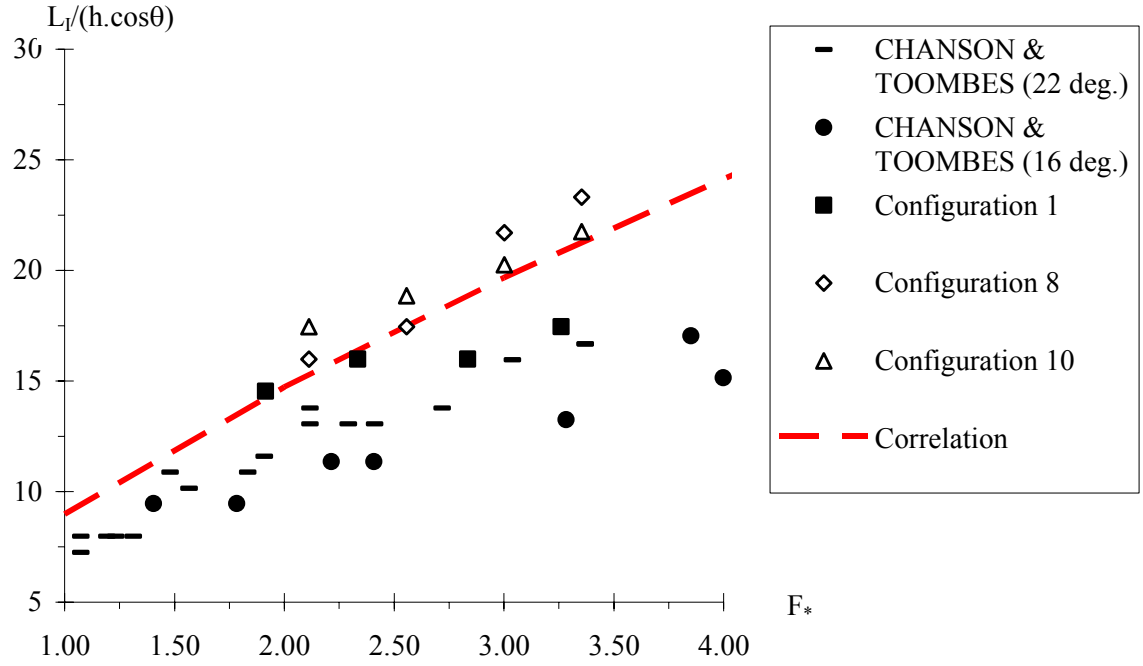

Cavity recirculation in skimming flows

Downstream of the point of inception, the air-water skimming flow is fully developed and strong exchanges of air-water and momentum occur between the main stream and the atmosphere. Intense cavity recirculation is also observed below the pseudo-invert formed by the step edges. Three-dimensional cavity vortices develop beneath the mainstream. It is believed that these vortices are maintained through the transmission of momentum from the main stream. Skimming flows are characterised by very significant form losses (Rajaratnam 1990, Chanson et al. 2002, Gonzalez and Chanson 2004).

For the stepped chute configurations 2 to 7 with vanes placed across the step cavities, visual observations from the sidewall showed some effects of the longitudinal ribs on the recirculation vortices and on the main stream. The cavity recirculation seemed to be similar in period and phase to the cavity fluid ejections

observed in d-type roughness (Djenidi et al. 1999) and in stepped chute flows. The recirculation vortices appeared to place strong pressures and cause shear forces on the triangular ribs. For the rough step configurations 8 to 10, the observations suggested some different flow patterns in the recirculation zones beneath the main stream. For chutes with rough steps the location of the inception point shifted downstream. Additionally, more aerated cavities were consistently observed upstream of the point of inception for configuration 8 than for the other configurations (Gonzalez et al. 2005). Downstream of the inception point, recirculating eddies with clear water cores in the step corners were seen in Configurations 8 and 10, while the whole cavity regions were fully-aerated in the chutes for configuration 9 and configurations 1 to 7. This is illustrated in Figure 5.

Fig. 5 - Photographs of recirculation cavities for rough step configurations
(A) Configuration 8 (B) Configuration 9

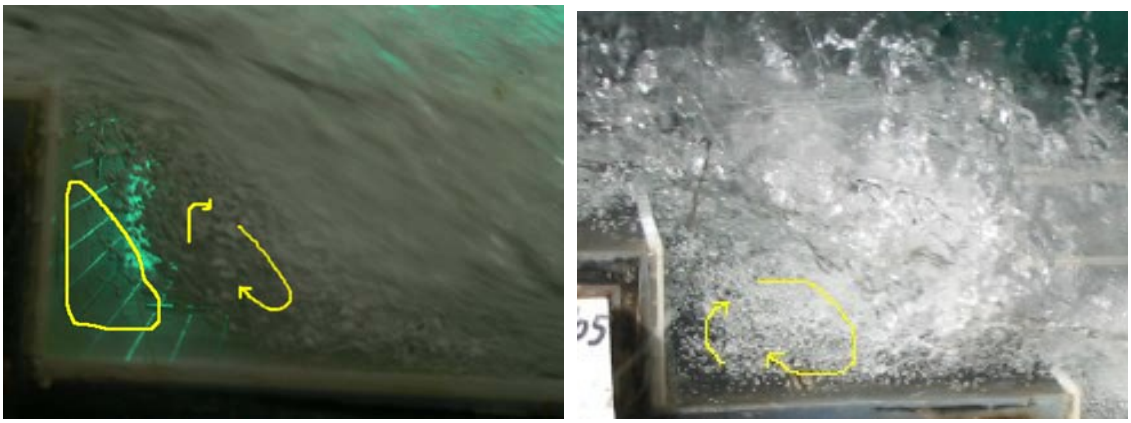

Air-water flow properties

A detailed comparison of the air-water flow properties for all tested configurations was conducted. Figure 6 present some results. In Figure 6, the data were obtained for the same flow conditions ($d_c/h \approx 1.39$) at step edges and at identical dimensionless distances from the inception point $(x-L_I)/L_{cav} = 2$ where L_I is the length to the point of inception and L_{cav} is the cavity length. The data corresponding to vane configurations (2 to 7) were recorded at a transverse distance of z/b = 0.25. Figure 6 presents dimensionless results in terms of air concentration C, velocity V/V_{90}, turbulence Tu and bubble count rate $F.d_c/V_c$ distributions for all tested configurations where y is the distance normal to the pseudo-bottom formed by the step edges, Y_{90} is the distance where C = 0.90 and V_{90} is the air-water flow velocity at $y = Y_{90}$. The data legend is given in Table 2. The air concentration data measured at step edges were similar for all configurations suggesting negligible effects of the vanes and step roughness on the rate of air entrainment. In Figure 6B, the void fraction distributions are compared successfully with an analytical solution of the air bubble diffusion equation :

$$C = 1 - \tanh^2\left(K' - \frac{y'}{2 * D_o} + \frac{\left(y' - \frac{1}{3}\right)^3}{3 * D_o}\right) \quad [6]$$

where $y' = y/Y_{90}$ (Chanson and Toombes 2002). D_o and K' are dimensionless functions of the mean air concentration C_{mean}:

$$K' = 0.327 + \frac{1}{2 * D_o} - \frac{8}{81 * D_o} \quad [7]$$

$$C_{mean} = 0.762 * (1.043 - \exp(-3.61 * D_o)) \quad [8]$$

with

$$C_{mean} = \int_0^1 C * dy' \quad [9]$$

Figure 6B presents a comparison between all the velocity data and a $1/7^{th}$ power law. The velocity data for each vane configuration showed some velocity defect region above the longitudinal ribs for $y/Y_{90} < 0.5$ to 0.7, suggesting some wake developing above each rib. These results showed that the effect of the vanes was not limited to the cavity flow but extended into the mainstream. The velocity distribution data showed further some faster flows on rough stepped chutes, especially for the configurations 8 and 10. Although this finding might be counter-intuitive, it was consistently observed for all investigated discharges, and the present results yielded :

V/V_c [rough steps] > V/V_c [smooth steps] > V/V_c [vanes]

Figure 6C presents some turbulence level Tu distributions obtained for all configurations. The turbulence data showed high values for all vane configurations, while the turbulence levels on rough stepped chute were observed to be consistently lower than those on smooth stepped chutes and with vanes.

Fig. 6 - Air-water flow properties on embankment dam stepped chute ($d_c/h = 1.39$), $(x- L_I)/L_{cav} = 2$

(A) Air concentration C

(B) Air-water velocity V/V_{90}

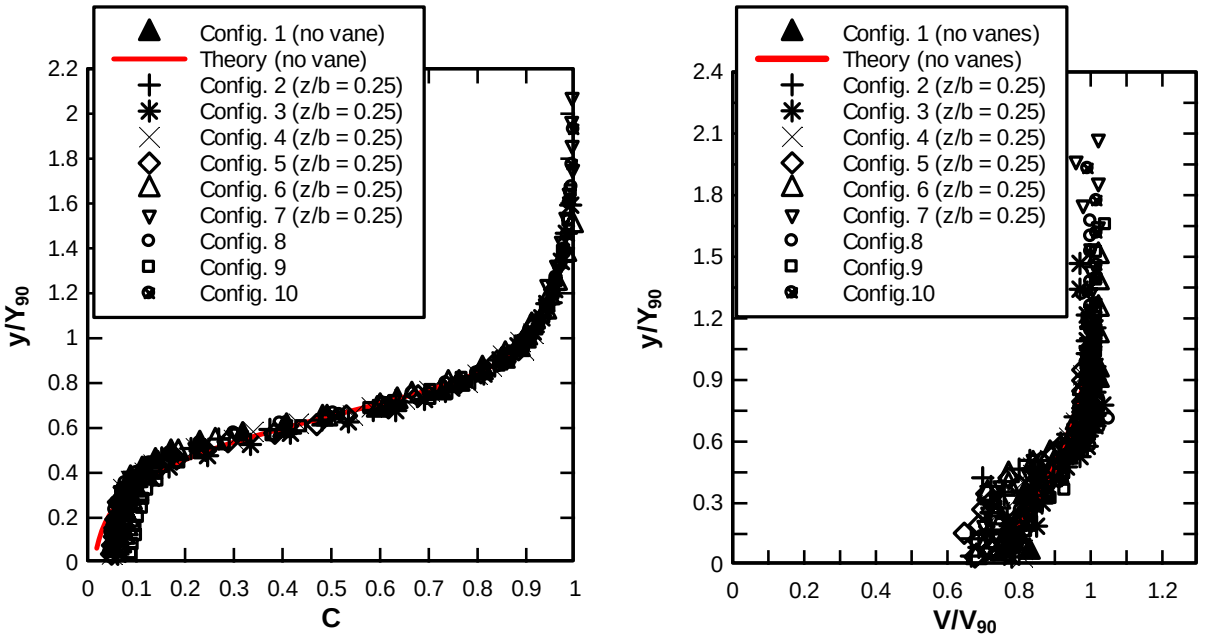

(C) Turbulence level Tu

(D) Bubble count rate $F.d_c/V_c$

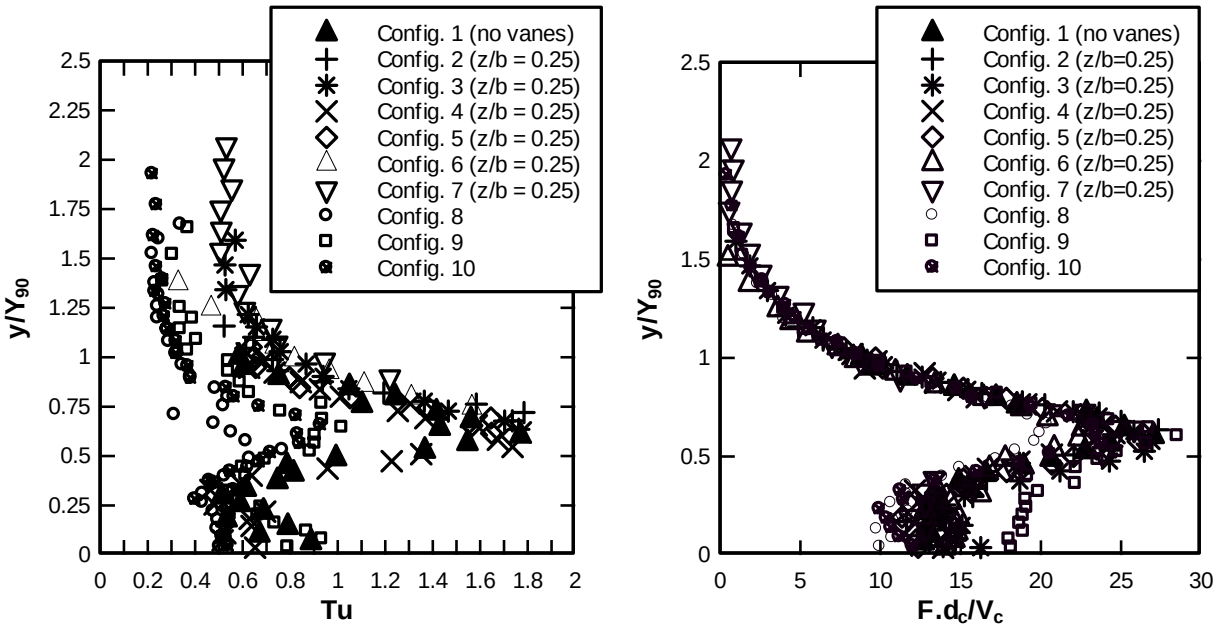

Table 2 - Legend for Figures 6 and 7

Symbol	Description	Symbol	Description
□	Configuration 1 (No vanes)	●	Configuration 7 (vanes)
◇	Configuration 2 (vanes)	∗	Configuration 8 (rough steps)
▲	Configuration. 3 (vanes)	▲	Configuration 9 (rough steps)
+	Configuration. 4 (vanes)	×	Configuration 10 (rough steps)
△	Configuration 5 (vanes)	–––	Theory (no vanes)
◆	Configuration 6 (vanes)		

Energy dissipation

In smooth channels, the kinetic energy dissipation occurs predominantly through friction losses. On stepped cascades, some additional dissipation mechanisms exist including cavity recirculation vortices beneath the mainstream, momentum exchange between main flow stream and mixing layer formed downstream of each step edge, and skin friction at the downstream half of the steps. Altogether these mechanisms cause some very significant form drag.

Despite their limitations, the Darcy-Weisbach friction factor was used to estimate the form losses in the stepped channel because it is still widely used for open channel design (Henderson 1966, Chanson 19999). For an uniform equilibrium flow in a wide channel, the boundary friction counteracts the gravity force component in the flow direction and the flow depth and velocity may be determined from the momentum principle :

$$\tau_o \times P_w = \rho_w \times g \times A_w \times \sin\theta \qquad [10]$$

where τ_0 is the average shear stress between the skimming flow and the recirculating fluid underneath, P_w is the wetted perimeter, A_w is the water flow cross-section area and θ is the mean bed slope.

In gradually-varied flows, the flow resistance may be calculated from the average friction slope S_f (Chanson et al. 2002). Experimental results are presented in terms of the Darcy friction factor f_e in Figure 7 for all configurations, where:

$$f_e = \frac{8 \times g}{q_w^{\,2}} \times \left(\int_{y=0}^{Y_{90}} (1-C) \times dy \right)^3 \times S_f \qquad [11]$$

For the configurations without ribs (1, 8, 9 and 10), the friction factors f_e were calculated based upon measurements conducted at step edges on the channel centreline. For the configurations with longitudinal ribs, f_e was estimated as a transverse-averaged value based upon measurements at three transverse positions above and between the vanes. Figure 7 compares the flow resistance data. The experimental values obtained in two stepped channels (θ = 11.3 & 19°) with different step heights (h = 0.025, 0.0393, 0.05 & 0.0785 m) by Yasuda and Ohtsu (1999) are also presented for comparison.

For smooth steps, the equivalent Darcy-Weisbach friction factor was about $f_e = 0.16$ that is consistent with earlier analyses yielding $f_e \sim 0.2$ (Chanson et al. 2002, Chanson 2006). The largest friction factors were observed for the configurations with vanes in zigzag (Config. 3 and 5) and the lowest flow resistance was

observed for the configurations with rough screens on the horizontal step faces (Config. 8 and 10) : $(f_e)_{rough} \approx 0.12$ in average. Overall, the findings suggested that the longitudinal ribs increased the flow resistance and the rate of energy dissipation. Contrarily to intuition, the rough screens on the step faces did not further flow resistance.

Fig. 7 - Flow resistance estimates in skimming flows on embankment stepped chutes - Legend as per Table 2, except for the symbols "o" denoting the data of Yasuda and Ohtsu (1999) for θ =11 and 19°

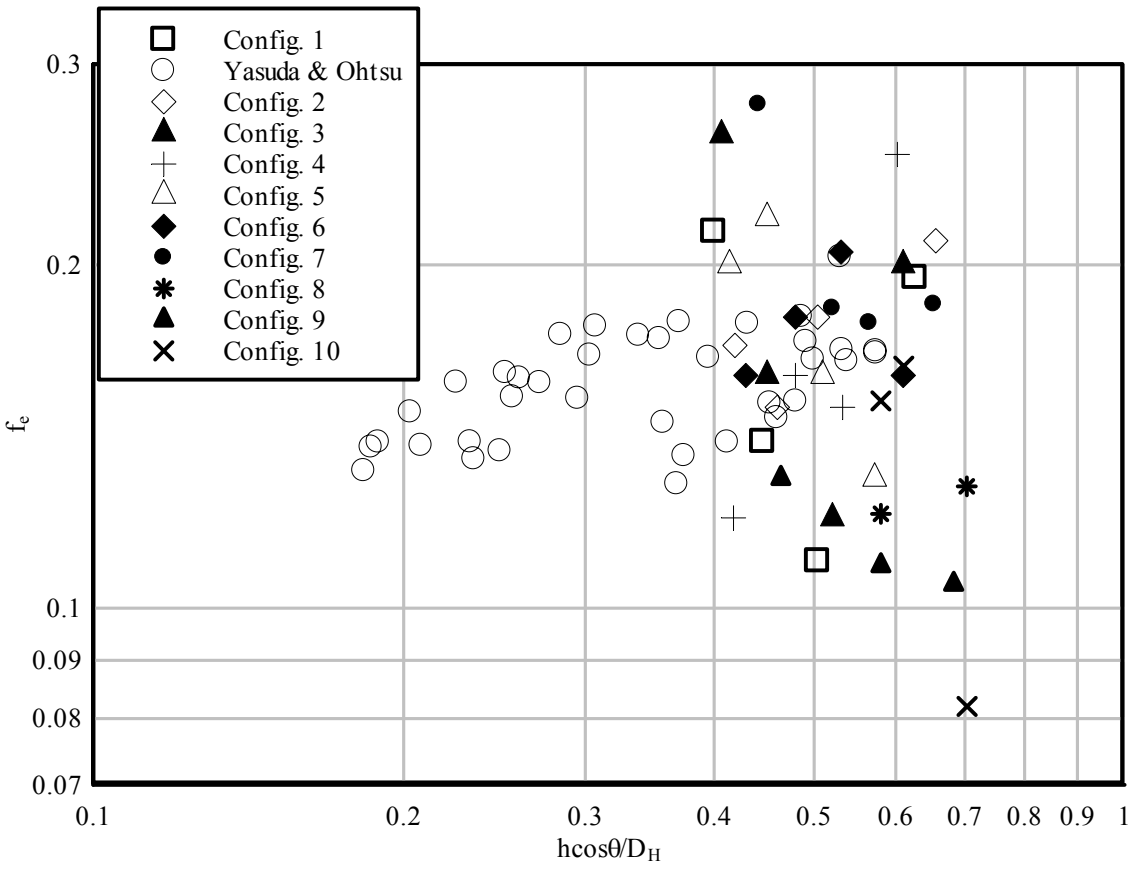

Design criterion

Despite the increasing popularity of moderate slope stepped chutes, most studies and design criterions are limited to steep chutes ($\theta \approx 30$ to 50^o). Only two design criterions discussed the hydraulic performance of stepped cascades with flat to moderate slopes ($11^o < \theta < 30^o$; Chanson 2001, Ohtsu et al. 2004). There are still a number of key issues not well understood, and design criteria need to be improved, specifically in terms of flow resistance and energy dissipation. The present design method can be used for moderate slope chutes ($10^o < \theta < 25^o$) with skimming flows at design conditions ($1.0 < d_c/h < 3.2$).

The skimming flow regime is recommended to pass large water discharges while nappe flow is best to achieve maximum energy dissipation rate on short stepped cascades. The transition flows should be avoided as they might produce dangerous dynamic loads to the structure. Note that it is important that the designers account not only for the design flow rate but also some smaller flow conditions.

When designing a stepped spillway, the dam height, the downstream slope of the dam and the design discharge are generally given. The variable parameters may include the type of flow and the step height. However, the designer is often limited to select a step height (h) within the values determined by the dam construction technique (h = 0.2 to 0.9 m with RCC or gabions).

The first step is to calculate the critical depth at the crest.

$$d_c = \sqrt[3]{\frac{Q_w^2}{g \cdot W^2}} \qquad [12]$$

Secondly, the step height should be selected to ensure that the chute will operate with skimming flow conditions (Fig. 3).

The location of the point of inception should be located to ensure that free-surface flow aeration occurs in the upstream end of the chute to achieve fully-developed flow conditions before the toe of the chute. Its coordinates might be calculated as:

$$\frac{L_I}{h\cos\theta} = 9.719 \sin\theta^{0.0796} \left(\frac{q_w}{\sqrt{g \sin\theta (h\cos\theta)^3}} \right)^{0.713} \qquad [13]$$

$$\frac{d_I}{h\cos\theta} = \frac{0.4034}{(\sin\theta)^{0.04}} \left(\frac{q_w}{\sqrt{g \sin\theta (h\cos\theta)^3}} \right)^{0.592} \qquad [14]$$

where L_I and d_I are the length to and depth at the inception point (Chanson 1995). Note that fully developed condition must preferably be achieved before the toe of the stepped chute :

$$\frac{d_c}{h} < \frac{1}{0.1193 \cdot \cos\theta \times \sin\theta^{0.259} \times \left(\frac{L}{h \cdot \cos\theta}\right)^{0.935}} \quad [15]$$

However this is not always possible (See discussion below).

Designers must also consider a maximum value of d_c/h above which the steps become too small and no longer act as a large roughness. Chanson (2001) suggested a maximum step height limit of:

$$h \leq 15 \cdot d_c \cdot \cos\theta \quad [16]$$

After this point, designers may follow different paths depending if the chute is long enough to achieve uniform equilibrium (normal) flow conditions.

If the channel is long enough for the flow to reach uniform equilibrium, the characteristic flow depth d should be calculated as:

$$d = d_c \cdot \sqrt[3]{\frac{f_e}{8 \cdot \sin\theta}} \quad [17]$$

where f_e is the Darcy friction factor estimated based upon experimental air-water flow friction factor data as suggested by Chanson et al. (2002) and Chanson (2006). In air-water flows, the friction factors f_e decrease with increasing mean air concentration C_{mean}, hence f_e should be calculated as:

$$\frac{f_e}{f_m} = 0.5 \cdot \left(1 + \tanh\left(2.5 \cdot \frac{0.5 - C_{mean}}{C_{mean} \cdot (1 - C_{mean})}\right)\right) \quad [18]$$

where f_m should be deduced with Equation [10] and the average C_{mean} might be computed based upon a criterion developed by Ohtsu et al. (2004):

$$C_{mean} = D - 0.3 \cdot e^{\left\{-5 \cdot \left(\frac{h}{d_c}\right)^2 - 4 \cdot \left\{\frac{h}{d_c}\right\}\right\}} \quad [19]$$

where D = 0.3 for $5.7^o < \theta < 19^o$, $D = -0.00024\theta^2 + 0.0214\theta - 0.0357$ for $\theta \geq 19^o$. Finally, based on the obtained depth, the flow velocity ($U_w = q_w/d$), Y_{90} and the height of the sidewalls h_w can be estimated ($h_w = 1.4 \times Y_{90}$).

If the flow does not reach normal flow conditions before the toe of the chute, the air-water flow depth should be deduced from the integration of the backwater equation :

$$S_f = -\frac{\partial H}{\partial x} = \sqrt{\frac{f_e}{8}} \cdot \frac{q_w^2}{g \cdot d^3} \quad [20]$$

Several researchers have attempted to use the backwater equation to calculate water depth and Darcy friction factors making gross assumptions violating basic principles as it is only valid for smooth chute flows (Chanson 2001). This method is tedious and may not be suitable for all cases.

Alternatively the flow properties in the gradually varied flow region may be calculated with a correlation curve linking some well-documented experimental results with the theoretical calculations in the developing and equilibrium flow regions (Gonzalez 2005) :

$$\frac{U_w}{V_{max}} = 0.00107 \cdot \left(\frac{H_{max}}{d_c}\right)^2 - 0.0634 \cdot \left(\frac{H_{max}}{d_c}\right) + 1.202 \quad [21]$$

where H_{max} is the upstream total head, d_c is the critical depth, V_{max} is the ideal flow velocity and U_w is the downstream velocity (Fig. 8). In Equation [21], U_w is the unknown variable , H_{max} and d_c are known, V_{max} is estimated from Equations [22] or [23]. Once the dimensionless downstream velocity U_w/V_{max} is known, the flow properties can be estimated assuming fully developed flow conditions. The friction factor in skimming flow is typically $f_e = 0.2$. Finally, the ideal fluid flow velocity can be estimated from the Bernoulli equation:

$$V_{max} = \sqrt{2 \times g \times (H_{max} - d \times \cos\theta)} \quad [22]$$

with $d = q_w/U_w$. For a large structure, the ideal fluid flow velocity is simply:

$$V_{max} \approx \sqrt{2 \times g \times H_{max}} \quad [23]$$

Once, the velocity and depth of the flow are obtained, the average air concentration $C_{mean,}$ Y_{90} and the height of the sidewalls h_w can be computed ($h_w = 1.4 \times Y_{90}$).

This alternate method may be used for preliminary design calculations. However it is important to note that it was obtained assuming $f_e = 0.2$ as in the uniform equilibrium region and it was only validated for skimming flow in stepped chutes with moderate slopes ($15^o < \theta < 25^o$).

Designers should be aware that the embankment overflow stepped spillway design is a critical process, as any failure can lead to a catastrophe. A number of key parameters should be assessed properly, including stepped face erosion, seepage through the embankment, drainage beneath the steps, interactions between the abutments and the stepped face ... (Chanson and Gonzalez 2004). In turn, some physical modelling with scaling ratios no greater than 3:1 is strongly advised.

Fig. 8 - Sketch of an embankment dam stepped spillway

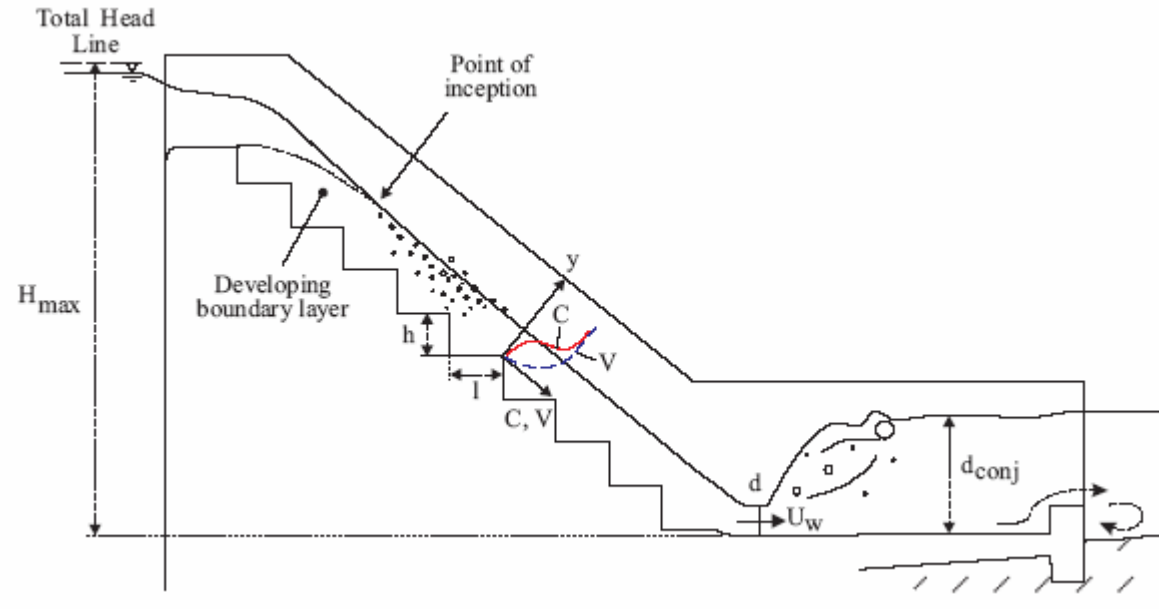

Discussion : design of small embankment dam spillways

For short stepped chutes and large discharges, the flow may not be fully-developed before the downstream of the chute. That is, the chute length may be smaller than the distance between crest and inception point. Chanson (1999, 2001) developed a simple method to predict the depth-averaged velocity and flow depth.

In the developing flow region, the flow consists of a turbulent boundary layer next to the invert and an ideal-fluid flow region above. In the ideal-fluid region ($\delta < y < d$), the velocity, called the free-stream velocity, is deduced from the Bernoulli equation :

$$V_{max} = \sqrt{2 \times g \times (H_{max} - d \times \cos\theta)} \qquad \text{Ideal fluid flow } (\delta < y < d) \quad [24]$$

where H_{max} is the upstream total head, θ is the channel slope, d is the flow depth and δ is the boundary layer thickness. In the boundary layer, experimental data indicate that the velocity distribution follows closely a power law :

$$\frac{V}{V_{max}} = \left(\frac{y}{\delta}\right)^{1/N} \qquad 0 < y/\delta < 1 \quad [25]$$

where y is the distance normal to the channel bed. The velocity distribution exponent equals about N = 5 for stepped chutes. Combining Equations [24] and [25], the continuity equation gives:

$$q_w = V_{max} \times \left(d - \frac{\delta}{N+1}\right) \qquad [26]$$

The boundary growth in skimming flow is enhanced by the turbulence generated by the steps. It may be estimated in first approximation :

$$\frac{\delta}{x} = 0.0301 \times \frac{1}{(\sin\theta)^{0.11}} \times \left(\frac{x}{h \times \cos\theta}\right)^{-0.17} \qquad [27]$$

where h is the step height and x is the curvi-linear coordinate along the flow direction from the crest. Equation [27] was checked with model and prototype data (e.g. Chanson 1995, Meireles et al. 2006).

At a distance x from the crest, Equation [27] provides an estimate of the boundary layer thickness δ, and the flow depth d is given by Equation [26]. The depth-averaged velocity is then : $U_w = q_w/d$.

Conclusion

Flows cascading down a stepped spillway with a moderate slope are characterised by some strong aeration and high turbulence of the flow. An experimental study was conducted herein based on Froude similitude in large-size experimental facilities to gain a better understanding of the flow properties in stepped chutes with slopes typical of embankment dams. A total of 10 configurations were tested including smooth steps, steps equipped with devices to enhance energy dissipation and rough steps. The results included air water flow properties such as air concentration, flow velocity, turbulence, and bubble count rate. Based on measured air-water velocities, the flow resistance was estimated accurately. The equivalent Darcy-Weisbach friction factors for moderate slope stepped chutes were larger than those for smooth chutes which averaged a value of $f_e \sim 0.2$. In addition some scale effects were observed in terms of bubble count rate, turbulence intensity and flow resistance.

The present results yielded a new design criterion. Although the study is based on limited experimental data, the criterion assessed some key issues not foreseen in prior studies : e.g., gradually varied flow, type of flow regime, flow resistance. While the findings were obtained for two moderate slopes (θ = 16 and 22º), it is believed that the outcomes are valid for a wider range of chute geometry and flow conditions typical of embankment chutes.

Acknowledgements

The writers acknowledge the helpful comments of Dr John Macintosh (Water Solutions), the technical assistance of Graham Illidge and Clive Booth (The University of Queensland). The first writer thanks the financial support of the National Council for Science and Technology of Mexico (CONACYT).

References

Andre, S., Boillat, J.L., Schleiss, A.J., and Matos, J. (2004). "Energy Dissipation and Hydrodynamic Forces of Aerated Flow over Macro-Roughness Linings for Overtopped Embankment Dams." *Proc. Intl Conf. on Hydraulics of Dams and River Structures*, Tehran, Iran, Balkema Publ., The Netherlands, pp. 189-196.

Chamani, M.R., and Rajaratnam, N. (1999). "Characteristics of Skimming Flow over Stepped Spillways." *Jl of Hyd. Engrg.*, ASCE, Vol. 125, No. 4, pp. 361-368. Discussion : Vol. 126, No. 11, pp. 860-872. Closure : Vol. 126, No. 11, pp. 872-873.

Chanson, H. (1995). "Hydraulic Design of Stepped Cascades, Channels, Weirs and Spillways." *Pergamon*, Oxford, UK, Jan., 292 pages.

Chanson, H. (1999). "The Hydraulics of Open Channel Flows : An Introduction." *Edward Arnold*, London, UK, 512 page.

Chanson, H. (2001). "The Hydraulics of Stepped Chutes and Spillways." *Balkema*, Lisse, The Netherlands, 418 pages.

Chanson, H. (2006). "Hydraulics of Skimming Flows on Stepped Chutes: the Effects of Inflow Conditions?" *Jl of Hyd. Res.*, IAHR, Vol. 44, No. 1, pp. 51-60.

Chanson, H., and Gonzalez, C.A. (2004). "Stepped Spillways for Embankment dams: Review, Progress and Development in Overflow Hydraulics." *Proc. Intl Conf. on Hydraulics of Dams and River Structures*, Tehran, Iran, Balkema Publ., The Netherlands, pp. 287-294.

Chanson, H., and Toombes, L. (2002). "Air-Water Flows down Stepped chutes : Turbulence and Flow Structure Observations." *Intl Jl of Multiphase Flow*, Vol. 27, No. 11, pp. 1737-1761.

Chanson, H., and Toombes, L. (2002b). "Experimental Investigations of Air Entrainment in Transition and Skimming Flows down a Stepped Chute." *Can. Jl of Civil Eng.*, Vol. 29, No. 1, pp. 145-156.

Chanson, H., and Tombes, L. (2004). "Hydraulics of Stepped Chutes: the Transition Flow." *Jl of Hyd. Res.*, IAHR, Vol. 42, No. 1, pp. 43-54.

Chanson, H., Yasuda, Y., and Ohtsu, I. (2002). "Flow Resistance in Skimming Flows and its Modelling." *Can Jl of Civ. Eng.*, Vol. 29, No. 6, pp. 809-819.

Crowe, C., Sommerfield, M., and Tsuji, Y. (1998). "Multiphase Flows with Droplets and Particles." *CRC Press*, Boca Raton, USA, 471 pages.

Djenidi, L., Elavasaran, R., and Antonia, R.A. (1999). The Turbulent Boundary Layer over Transverse Square Cavities. *Jl Fluid Mech.*, Vol. 395, pp. 271-294.

Gonzalez, C.A. (2005)."An Experimental Study of Free-Surface Aeration on Embankment Stepped Chutes." *Ph.D. Thesis*, Dept. of Civil Engineering, University of Queensland, Brisbane, Australia.

Gonzalez, C.A., and Chanson, H. (2004). "Interactions between Cavity Flow and Main Stream Skimming Flows: an Experimental Study." *Can Jl of Civ. Eng.*, Vol. 31, No. 1, pp. 33-44.

Gonzalez, C.A., and Chanson, H. (2005). "Experimental Study of Turbulence Manipulation in Stepped Spillways. Implications on Flow Resistance in Skimming Flows." *Proc. 31st Biennial IAHR Congress*, Seoul, Korea, B.H. JUN, S.I. LEE, I.W. SEO and G.W. CHOI Editors, Theme D.7, Paper 0057, pp. 2616-2626.

Gonzalez, C.A., Takahashi, M., and Chanson, H. (2005). "Effects of Step Roughness in Skimming Flows: an Experimental Study." *Research Report No. CE160*, Dept. of Civil Engineering, The University of Queensland, Brisbane, Australia, July, 149 pages.

Henderson, F.M. (1966). "Open Channel Flow." *MacMillan Company*, New York, USA.

Manso, P.A., and Schleiss, A.J. (2002). "Stability of Concrete Macro-Roughness Linings for Overflow Protection of Earth Embankment Dams." *Can Jl of Civil Eng.*, Vol. 29, No. 5, pp. 762-776.

Meireles, I, Cabrita, J., and Matos, J. (2006). " Non-Aerated Skimming Flow Properties on Stepped Chutes over Embankment Dams." *Proceedings of the International Junior Researcher and Engineer Workshop on Hydraulic Structures (IJREWHS'06)*, Montemor-o-Novo, Jorge Matos and Hubert Chanson Eds., Report CH61/06, Div. of Civil Engineering, The University of Queensland, Brisbane, Australia, Dec., pp 91-99.

Ohtsu, I., Yasuda, Y., and Takahashi, M. (2004). "Flow Characteristics of Skimming Flows in Stepped Channels." *Jl of Hyd. Engrg.*, ASCE, Vol. 130, No. 9, pp. 860-869.

Peyras, L., Royet, P., and Degoutte, G. (1991). "Ecoulement et Dissipation sur les Déversoirs en Gradins de Gabions." ('Flows and Dissipation of Energy on Gabion Weirs.') *Jl La Houille Blanche*, No. 1, pp. 37-47 (in French).

Rajaratnam, N. (1990). "Skimming Flow in Stepped Spillways." *Jl of Hyd. Engrg.*, ASCE, Vol. 116, No. 4, pp. 587-591. Discussion : Vol. 118, No. 1, pp. 111-114.

Wood, I.R., Ackers, P., and Loveless, J. (1983). "General Method for Critical Point on Spillways." *Jl. of Hyd. Eng.*, ASCE, Vol. 109, No. 2, pp. 308-312.

Yasuda, Y., and Ohtsu, I.O. (1999). "Flow Resistance of Skimming Flow in Stepped Channels." *Proc. 28th IAHR Congress*, Graz, Austria, Session B14, 6 pages.